Bol. Soc. Paran. Mat.
©SPM –ISSN-2175-1188 ON LINE
SPM: www.spm.uem.br/bspm

(3s.) **v. ???? (??)** : 1–20.
ISSN-0037-8712 IN PRESS
doi:10.5269/bspm.64110

Numerical Method of the Exact Control for the Elastic String Problem with Moving Boundary *

Carla E. O. de Moraes, Mauro A. Rincon* and Gladson O. Antunes

ABSTRACT: The objective of this article is to investigate, analytically and numerically, the exact control problem associated with a mathematical model that describes the vertical vibrations of elastic strings, with moving contours. To determine the approximate numerical solution, following the description of the HUM (Hilbert Uniqueness Method), the finite element method associated with the Newmark method was used for the adjunct problem and the backward problem. To calculate the optimal control, the conjugated gradient method is used. The properties of a numerical problem must be consistent with the theoretical mathematical one. However, in order to obtain the numerical control, the grid is of fundamental importance, so we used the Bi-Grid technique. In this way, we developed an algorithm to solve this problem. Numerical simulations were performed for different initial data and moving contours, with and without the Bi-Grid algorithm and the numerical results confirmed the consistency between the theoretical and numerical results.

Key Words: Exact control, elastic string, Moving boundary, HUM method, numerical simulation, bi-Grid method.

Contents

1. Introduction and Problem Formulation

Let $\alpha_0 < \beta_0$ be the ends of an elastic string on the x axis, with $a < \alpha_0 < \beta_0 < b$, a, b fixed. We suppose that these ends move continuously to the position $\alpha(t) < \alpha_0$ and $\beta_0 < \beta(t)$, where $a \leq \alpha(t) < \beta(t) \leq b$. For $T > 0$, we denote by $\hat{Q}$ the non cylindrical domain on $\mathbb{R}^2$ defined by:

$$\hat{Q} = \{(x,t) \in \mathbb{R}^2;\ \alpha(t) < x < \beta(t),\ \forall t \in (0,T)\},$$

with lateral boundary $\hat{\Sigma} = \hat{\Sigma}_{0t} \cup \hat{\Sigma}_{1t}$, where:

$$\hat{\Sigma}_{0t} = \{(t, \alpha(t)), \forall t \in (0,T)\} \quad \text{and} \quad \hat{\Sigma}_{1t} = \{(t, \beta(t)), \forall t \in (0,T)\}.$$

* The corresponding author M. A. Rincon is partially supported by CNPQ- Brazil and FAPERJ- Brazil
2010 *Mathematics Subject Classification:* 65M60, 65M55, 35R37, 35L10, 93C20.
Submitted June 22, 2022. Published September 04, 2022

We want to study the exact control problem associated to the following model:

$$\begin{cases} u'' - \Big(\dfrac{\tau_0}{m} + \dfrac{k}{m}\dfrac{\gamma(t)-\gamma_0}{\gamma_0}\Big)u_{xx} + f(u) = 0 \quad \text{in} \quad \hat{Q}, \\ \\ u = \begin{cases} \varphi & \text{on} \quad \hat{\Sigma}_{0t} \\ 0 & \text{on} \quad \hat{\Sigma}_{1t}, \end{cases} \\ \\ u(0) = u_0, \qquad u'(0) = u_1 \text{ in }]\alpha_0, \beta_0[, \end{cases} \tag{1.1}$$

where $\gamma(t) = \beta(t) - \alpha(t)$ is the length of the string at each instant and $\tau(0) = \tau_0$ is the initial tension of the string, m is its mass, $k = k(m)$ is a constant that depends on the material of the string, $\alpha_0 = \alpha(0)$, $\beta_0 = \beta(0)$, $\gamma_0 = \gamma(0)$, the term $\Big(\dfrac{\tau_0}{m} + \dfrac{k}{m}\dfrac{\gamma(t)-\gamma_0}{\gamma_0}\Big)$ is positive, $u'' = \partial^2 u/\partial t^2$ and $u_{xx} = \partial^2 u/\partial x^2$.

The equation in (1.1), without the resistance represented by $f(u)$, is a linearization of Kirchhoff's equation for small vibrations of a stretched elastic string when the ends are variables, see [20]. In this paper, however, when dealing with numerical simulations in section 4 and on, we will consider f a linear function. For the reader interested in the theoretical aspects of the exact control problem for the problem (1.1), including the nonlinear case, we suggesting the reference [1].

An exact control problem can be formulated as: Consider an evolution system modeled by a differential equation. Given a time interval $(0, T)$, $T > 0$, and initial and final data of it, we want to obtain a control, that is, a function that acts over this system, in order to lead its solution from the initial state, at time $t = 0$, to the final state, at time $t = T$. The literature on the topic is vast. We can cite some texts that deal with this kind of problems analytically, as [2], [3], [5], [6], [18], [19], and also its references.

In special, we cite the reference [7] and [17] that deals with the internal and boundary exact controllability of some nonlinear hyperbolic systems with local and nonlocal nonlinearities in dimension one.

The exact boundary controllability study of $1-D$ parabolic and hyperbolic degenerate equations can be found in [15] and [16]. In addition to exact controllability, we can mention the recent works on null controllability [4], [7], [8] and [10], among others.

Throughout this article, we will cite other references and all of them prove that this field has been studied a lot and that there are still many problems to be solved.

In practice, control problems need to be implemented, and therefore approximated, through algorithms and numerical simulations. From the numerical point of view, many studies have been made recently and, in particular, studies on the hyperbolics equations: [3], [9], [23] and [24]. In [25] the numerical solution for the problem of exact controllability of linear Korteweg-de Vries (KdV) equation was obtained using the Spectral method and the problem of numerically computing the exact boundary control for the linear elasticity system in two dimensions was developed in [11].

Numerical results must be consistent with theoretical results. However, not all number schemes can achieve this goal. A natural way one can think of to solve control problems numerically is to approximate the given system using discrete (or semi-discrete) schemes, and obtain the control as the limit of the sequence of successive controls, corresponding to the approximated equations. However, according to [3], for most numerical schemes, when doing it, some important properties can be lost when the spatial discretization parameter tends to zero. In this way, it is necessary to complement in some way the theory of the numerical method. To overcome this adversity, reestablishing the convergence of the approximation, some techniques have been proposed in the literature when dealing with the wave equation defined in a cylindrical domain, among them, we can mention: Tychonoff regularization [13], Mixed Finite Element Method [12] and Bi-Grid methods [14] and Conjugate Gradient Method.

The same techniques and arguments used in this paper can be applied in dimension 2 in the study of plates, for instance.

2. Equivalent Problem and Hypotheses

Consider the change of variables $u(x,t) = v(y,t)$, where $y = \left(\frac{x-\alpha(t)}{\gamma(t)}\right)$, as in [1,20]. This way, note that when (x,t) varies in $\hat{Q}$, (y,t) varies in $Q = (0,1)\times(0,T)$, as in Figure 1. The application $\tau : \hat{Q} \to Q, \quad \tau(x,t) = \left(\frac{x-\alpha(t)}{\gamma(t)}, t\right) = (y,t)$ and its inverse are of class C^2, according to [20].

Besides, application τ transforms the equation $(1.1)_1$ into the equivalent one:

$$v'' - [a(y,t)v_y]_y + b(y,t)v'_y + c(y,t)v_y + f(v) = 0,$$

where:

$$a(y,t) = \left(\frac{\tau_0}{m} + \frac{k}{m}\frac{\gamma(t)-\gamma_0}{\gamma_0}\right)\frac{1}{\gamma^2(t)} - \left(\frac{\alpha'(t)+\gamma'(t)y}{\gamma(t)}\right)^2, \tag{2.1}$$

$$b(y,t) = -2\left(\frac{\alpha'(t)+\gamma'(t)y}{\gamma(t)}\right), \tag{2.2}$$

$$c(y,t) = -\frac{\alpha''(t)+\gamma''(t)y}{\gamma}. \tag{2.3}$$

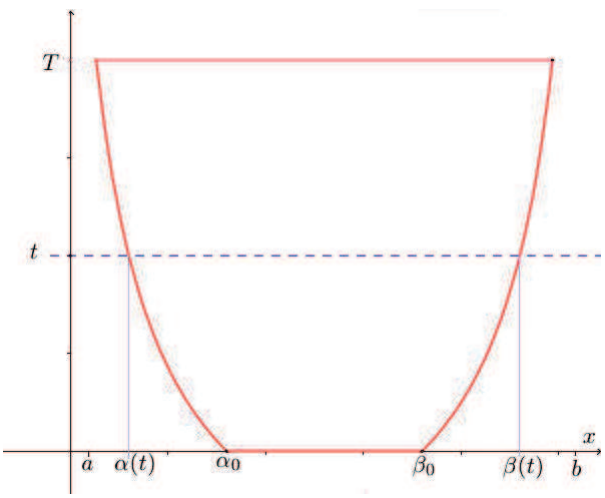

Figure 1: Domain and boundary moving

So, it is enough to study the exact controllability for the equivalent problem, that is:

$$\begin{cases} v'' - (a(y,t)v_y)_y + b(y,t)v'_y + c(y,t)v_y + f(v) = 0, & \text{in} \quad Q, \\ v(0,t) = w(t), \qquad v(1,t) = 0 \qquad \text{in } (0,T), \\ v(y,0) = v_0(y), \qquad v'(y,0) = v_1(y) \text{ in } (0,1), \end{cases} \tag{2.4}$$

where $w \in L^2(0,T)$ is the control.

In order to deal with (2.4) analytically, we need the following hypotheses:

$$\alpha, \beta \in W^{3,1}((0,\infty)) \cap W^{3,\infty}_{loc}((0,\infty)), \ \ \alpha(t) < \beta(t), \ \ \alpha'(t) < 0 < \beta'(t), \forall t \in [0,T]. \tag{2.5}$$

$$|\alpha'(t) + \gamma'(t)y| \leq \left(\frac{\tau_0}{2m}\right)^{\frac{1}{2}}, \quad \forall (y,t) \in Q. \tag{2.6}$$

$$|\alpha''(t) + \gamma''(t)y| < \frac{|\alpha'(t)+\gamma'(t)y|^2}{\gamma(t)}, \quad \forall (y,t) \in Q. \tag{2.7}$$

$$f' \in L^\infty(\mathbb{R}), \quad \exists \lim_{|s|\to\infty} \frac{f(s)}{s} = \sigma. \tag{2.8}$$

According to [1], there exists a unique global solution for (2.4), and therefore there exists a unique global solution for (1.1).

3. Mathematical Aspects

We are interested in studying the exact controllability of (2.4). In particular, in this paper, consider $f(s) = \sigma s, \forall s \in \mathbb{R}$ and $\sigma \in \mathbb{R}$ fixed. That is, in this study, from this point on, we will discuss the case where f is a linear function.

Define:

$$k_0 = \frac{\tau_0 \gamma_0^2}{32m(b-a)^2} > 0. \tag{3.1}$$

Theorem 3.1. *Assume (2.5), (2.6), (2.7) and (2.8) are satisfied. Let $T > 2/\sqrt{k_0}$, where k_0 is given by (3.1), then for every pair of initial data $\{v_0, v_1\} \in H^{-1}(0,1) \times L^2(0,1)$, there exists a unique control $w \in L^2(0,T)$ such as the solution $v = v(y,t)$ of (2.4) satisfies:*

$$v(y,T) = v'(y,T) = 0 \quad in \quad (0,1). \tag{3.2}$$

Proof: The proof can be found in [1] and it uses HUM (Hilbert Uniqueness Method). This method was presented in [18,19], and it can be considered a starting point to the development of the control theory over the past decades.

For the sake of making the reading of this paper more independent, we will give some details on the proof of this control result.

Based on (2.4), we define the operator $Lv(y,t)$ by:

$$Lv(y,t) = v''(y,t) - [a(y,t)v_y(y,t)]_y + b(y,t)v'_y(y,t) + c(y,t)v_y(y,t) + \sigma v(y,t).$$

So, from the definition of adjoint operator, we can conclude that the formal adjoint operator of L, denoted by L^*, is:

$$\begin{aligned} L^*z = z'' - [a(y,t)z_y]_y + b(y,t)z'_y + [b'(y,t) - c(y,t)]\, z_y + b_y(y,t)z' + \\ \left[b'_y(y,t) - c_y(y,t)\right] z + \sigma z. \end{aligned} \tag{3.3}$$

We observe that, due to the linearity and reversibility of the problem, we can consider the null final data.

Using these operators defined above, we can consider the following problems.

Adjoint Problem. Given $\{\phi_0, \phi_1\} \in \mathcal{D}(0,1) \times \mathcal{D}(0,1)$, we consider the problem:

$$\begin{cases} L^*\phi = 0 \quad \text{in} \quad Q, \\ \phi(0,t) = \phi(1,t) = 0 \qquad \text{on } (0,T), \\ \phi(y,0) = \phi_0(y), \qquad \phi'(y,0) = \phi_1(y) \text{ in } (0,1). \end{cases} \tag{3.4}$$

According to [21], problem (3.4) admits a unique solution ϕ with the regularity

$$\phi_y(0,t) \in L^2(0,T),$$

called hidden regularity.

Backward Problem. Using the solution of (3.4), we consider the problem:

$$\begin{cases} L\psi = 0 \quad \text{in} \quad Q, \\ \psi(0,t) = -\phi_y(t), \qquad \psi(1,t) = 0 \qquad \text{on } (0,T), \\ \psi(y,T) = \psi'(y,T) = 0 \text{ in } (0,1). \end{cases} \tag{3.5}$$

From the solution ψ of (3.5), define the operator Λ:

$$\{\phi_0, \phi_1\} \to \Lambda\{\phi_0, \phi_1\} = \{\psi'(0) + b(0)\psi_y(0), -\psi(0)\}. \tag{3.6}$$

Now, multiplying both sides of $(3.5)_1$ by ϕ and integrating in Q, we get:

$$\langle L\psi, \phi\rangle = -\langle \psi'(0) + b(0)\psi_y(0), \phi_0\rangle + (\psi(0), \phi_1) + \int_0^T a(0,t)|\phi_y(0,t)|^2 dt + \langle \psi, L^*\phi\rangle.$$

Note that $L\psi = L^*\phi = 0$ and from the definition of Λ, we conclude:

$$\langle \Lambda\{\phi_0, \phi_1\}, \{\phi_0, \phi_1\}\rangle = \int_0^T a(0,t)|\phi_y(0,t)|^2 dt. \tag{3.7}$$

Inspired by (3.7), we define in $\mathcal{D}(0,1) \times \mathcal{D}(0,1)$ the norm:

$$\|\{\phi_0, \phi_1\}\|_F^2 = \int_0^T a(0,t)|\phi_y(0,t)|^2 dt.$$

The operator Λ defined by (3.6) is linear and continuous with the norm $\|.\|_F$. And therefore, it has a unique extension to the closure of $\mathcal{D}(0,1) \times \mathcal{D}(0,1)$, with respect to $\|.\|_F$. Thus, the bilinear form defined by (3.7) is continuous and coercive in $F \times F$, which allows us to conclude, by Lax-Milgram's Theorem that the operator

$$\Lambda : F \longrightarrow F' \text{ is an isomorphism.}$$

Therefore, for $\{v_1, v_0\} \in F'$, there exists a unique $\{\phi_0, \phi_1\} \in F$ such that:

$$\Lambda\{\phi_0, \phi_1\} = \{v_1 + b(0)v_{0_y}, -v_0\} \in F'. \tag{3.8}$$

Comparing (3.6) with (3.8), we conclude that the unique solution of (3.5) satisfies (2.4). Therefore, the unique solution of (2.4), with control $w(t) = -\phi_y(0,t)$, verifies (3.2).

To complete the proof of controllability of (2.4), with $f(v) = \sigma v$, we have to characterize the spaces F and F' as being $H_0^1(0,1) \times L^2(0,1)$ and $H^{-1}(0,1) \times L^2(0,1)$, respectively. This is done by the direct and the inverse inequalities.

Direct Inequality. There exists a constant $C^* > 0$ such that:

$$C^* \int_0^T a(0,t)|\phi_y(0,t)|^2 dt \le \|\phi_0\|^2_{H_0^1(0,1)} + \|\phi_1\|^2_{L^2(0,1)}.$$

Inverse Inequality. Under the hypotheses of Theorem 3.1, there exists a constant $C^{**} > 0$ such that:

$$\|\phi_0\|^2_{H_0^1(0,1)} + \|\phi_1\|^2_{L^2(0,1)} \le C^{**} \int_0^T a(0,t)|\phi_y(0,t)|^2 dt.$$

The complete argument to prove the Direct and Inverse Inequalities can be seen in [1].

4. Numerical Method

As discussed in section 1, when dealing with control problems numerically, one has to complement the numerical method theory. Some techniques have been proposed in order to reestablish the convergence of the numerical control. Among them, we can cite the: Tikhonov regularization, mixed finite element method and Bi-Grid methods.

Problem:

$$\begin{cases} \phi''(y,t) - \left[a(y,t)\phi_y(y,t)\right]_y + b(y,t)\phi'_y(y,t) + \left[b'(y,t) - c(y,t)\right]\phi_y(y,t) + \\ \quad b_y(y,t)\phi'(y,t) + \left[b'_y(y,t) - c_y(y,t)\right]\phi(y,t) + \sigma\phi(y,t) = 0 \quad \text{in} \quad Q, \\ \phi(0,t) = \phi(1,t) = 0 \quad \text{on} \quad (0,T) \\ \phi(y,0) = \phi_0(y), \ \ \phi'(y,0) = \phi_1(y) \quad \text{in} \quad (0,1)\,. \end{cases}$$

Variational Problem: Take $V = H_0^1(0,1)$ and $\phi = \phi(y,t)$. Then, it holds:

$$(\phi'', v) - (\left[a(y,t)\phi_y\right]_y, v) + (b(y,t)\phi'_y, v) + (\left[b'(y,t) - c(y,t)\right]\phi_y, v) +$$

$$(b_y(y,t)\phi', v) + (\left[b'_y(y,t) - c_y(y,t)\right]\phi, v) + (\sigma\phi, v) = 0, \forall v \in V.$$

Integrating by parts, we obtain,

$$\begin{aligned} \therefore\ & (\phi'', v) + (a(y,t)\phi_y, v_y) + (b(y,t)\phi'_y, v) + (\left[b'(y,t) - c(y,t)\right]\phi_y, v) \\ & + (b_y(y,t)\phi', v) + (\left[b'_y(y,t) - c_y(y,t)\right]\phi, v) + \sigma(\phi, v) = 0, \forall v \in V. \end{aligned} \tag{4.1}$$

Faedo-Galerkin Method: Given $T > 0$. Let $V_m = [v_1, \ldots, v_m]$ be the subspace spanned by the first m basis vectors of the space V. If $\phi^h(y,t) \in V_m$, then it can be represented by:

$$\phi^h(y,t) = \sum_{i=1}^{m} d_i(t)v_i(x). \tag{4.2}$$

Restricting (4.1) to V_m and taking $v = v_j \in V_m$ and (4.2) in (4.1), we obtain:

$$\sum_{i=1}^{m} d_i''(t)(v_i, v_j) + \sum_{i=1}^{m} d_i(t)(a(y,t)v_{i_y}, v_{j_y}) + \sum_{i=1}^{m} d_i'(t)(b(y,t)v_{i_y}, v_j)$$

$$+ \sum_{i=1}^{m} d_i(t)(\left[b'(y,t) - c(y,t)\right]v_{i_y}, v_j) + \sum_{i=1}^{m} d_i'(t)(b_y(y,t)v_i, v_j)$$

$$+ \sum_{i=1}^{m} d_i(t)(\left[b'_y(y,t) - c_y(y,t)\right]v_i, v_j) + \sigma\sum_{i=1}^{m} d_i(t)(v_i, v_j) = 0.$$

Define the matrices:

$$A_{ij} = A_{ij}(t) = (a(y,t)v_{i_y}, v_{j_y}), \quad B_{ij} = B_{ij}(t) = (b(y,t)v_{i_y}, v_j),$$

$$H_{ij} = H_{ij}(t) = (\left[b'(y,t) - c(y,t)\right]v_{i_y}, v_j), \quad S_{ij} = S_{ij}(t) = (b_y(y,t)v_i, v_j),$$

$$P_{ij} = P_{ij}(t) = (\left[b'_y(y,t) - c_y(y,t)\right]v_i, v_j), \quad M_{ij} = (v_i, v_j).$$

Thus, it is true that:

$$\begin{cases} Md''(t) + Ad(t) + B^T d'(t) + H^T d(t) + Sd'(t) + Pd(t) + \sigma Md(t) = 0, \\ d(0) = d_0 = (\phi_0, v_j), d'(0) = d_1 = (\phi_1, v_j). \end{cases}$$

Defining $N = B^T + S$ and $R = A + H^T + P + \sigma M$, we have the following system of ordinary differential equations:

$$Md''(t) + Nd'(t) + Rd(t) = 0, \quad \forall t \in [0,T].$$

Now let's apply Newmark's method, to determine the approximate solution of the system of ordinary differential equations.

Consider the discretization of the fixed time interval $[0, T]$, using a uniform time step of size $\Delta t = T/N$, then $t_n = n\Delta t$, for $n = 0, 1, \cdots, N$ and $d^n = d(\cdot, t_n)$.

Newmark Method: Considering the parameters ζ and δ, from Taylor's expansion, it holds that:

$$\begin{cases} d_{n+1} = d_n + \Delta t d'_n + (\Delta t)^2 \left[\left(\frac{1}{2} - \zeta\right) d''_n + \zeta d''_{n+1} \right]. \\ d'_{n+1} = d'_n + \Delta t \left[(1-\delta) d''_n + \delta d''_{n+1} \right]. \end{cases}$$

We have already seen that $Md''(t_{n+1}) + Nd'(t_{n+1}) + Rd(t_{n+1}) = 0$, then using the above expansions, it holds that:

$$\left[M + \zeta(\Delta t)^2 R + \delta \Delta t N\right] d''_{n+1} = -N \left[d'_n + \Delta t(1-\delta) d''_n\right]$$

Therefore

$$-R\Big[d_n + \Delta t d' n + (\Delta t)^2 \big(0.5 - \zeta\big) d''_n\Big], \quad n = 0, 1, 2, \ldots$$

In particular, the basis we considered was formed by linear piecewise polynomial functions. A similar approach was used on the backwards problem. When dealing with derivatives, we used first and second order finite difference approximations. Further details can be found as comments on the program code.

Gradient Conjugate Method:

As already discussed in Section 3, the problem (3.8) , that is,

$$\Lambda\{\phi_0, \phi_1\} = \{v_1 + b(0) v_{0_y}, -v_0\},$$

admits a unique solution under the hypotheses of Theorem 3.1. Besides, note that (3.8) can be written in the variational form as follows: Find

$$\langle \Lambda\{\phi_0, \phi_1\}, \check{e}\rangle = \langle \{v_1 + b(0) v_{0_y}, -v_0\}, \check{e}\rangle, \forall \check{e} \in F. \tag{4.3}$$

Since the bilinear functional $\langle \Lambda., . \rangle$ is continuous, symmetric and coercive for T sufficiently large, then (4.3) has a unique solution that can be computed by the gradient conjugate method (see [13]).

The above notes are used in the implementation of the algorithm that will presented in Section 5. Before this, we will go over the Bi-Grid technique.

5. Bi-Grid Technique

Let $N \in \mathbf{N}$ be an odd number. Now, we will define two grids on the interval $(0, 1)$.

First, we define a fine grid such that, $h = 1/(N+1)$, $x_1 = h$, $x_N = 1-h$, $x_i - x_{i-1} = h, i = 2, \ldots, N+2$. That is, $x_i = ih$.

Then, we will also consider another partition of the interval $(h, 1-h)$, but now with step $2h$. That is, a grid that has nodes $y_1 = h, y_{(N-1)/2} = 1-h$, such that $y_j - y_{j-1} = 2h, j = 2, \ldots, (N-1)/2$. Note that this mesh is less refined (coarser) than the previous one.

In order to eliminate the known high frequencies that might produce unwanted oscillations, the Bi-Grid idea is to solve the adjoint and backward problems, considering a discretization in the fine grid, however the initial (or final) data will be taken in the less refined (coarse) one. So, it's necessary to define two operators so that we can solve these problems: an interpolation operator and a projection operator.

The interpolation operator, which we will denote by I^h_{2h}, will transform a vector data in the less refined grid into a vector data in the fine one as in Figure 2.

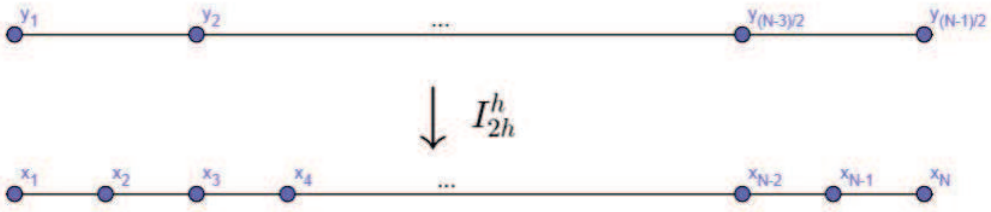

Figure 2: Interpolation Operator I_{2h}^{h}

So, we can take:

$$I_{2h}^{h} : R^{(N+1)/2} \longrightarrow R^{N}, \quad I_{2h}^{h}\, y = x,$$

where

$$x_{2i-1} = y_i, i = 1, \ldots, (N+1)/2; \quad x_{2i} = (y_i + y_{i+1})/2, i = 1, \ldots, (N-1)/2.$$

The goal of the projection operator, which we will denote by I_h^{2h}, is to transform a vector data in the fine grid to a vector data in the less refined grid, as in Figure 3.

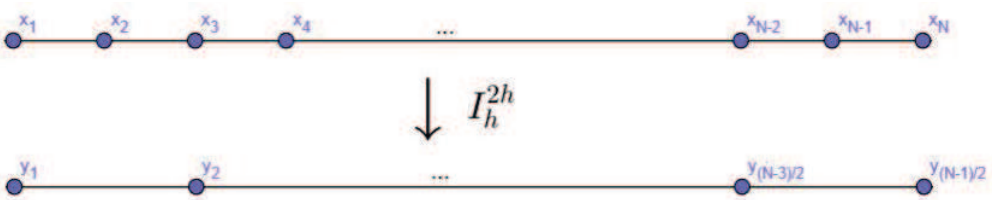

Figure 3: Projection Operator I_h^{2h}

Analogously, inspired by the algorithm implemented by the authors of [22], a possible choice is:

$$I_h^{2h} : R^{N} \longrightarrow R^{(N+1)/2}, \quad I_h^{2h}\, x = y,$$

where

$$y_i = x_{2i-1}, \quad i = 1, \ldots, (N+1)/2.$$

5.1. Algorithm

After studying this problem analytically and understanding the Bi-Grid technique as described above, we developed a program that will make possible obtain numerical simulations of it. Its algorithm can be found below.

Notation The indexes h and $2h$ indicate if the data will be taken on the fine or on the coarse grids, respectively. The index y indicates that we are referring to the derivative of the function with respect to y. We denote by ϕ and ψ the approximate solution of the adjoint and backward problems, respectively.

During Step 0, an abuse of notation is made when writing $I_h^{2h}(v_1)$ and $I_h^{2h}\left((v_0)_y\right)$. We will understand these as: the initial data of the main problem after the variable change v_0 and v_1 will be taken on the fine grid, initially. This way, it will be possible to apply the projection operator.

- Step 0: Initialization:
  - Choose a tolerance parameter $\varepsilon > 0$.

– Given any $e_0 = e_{0,2h}, e_1 = e_{1,2h}$ on the sparse grid, solve the following forward problem on the fine grid:

$$\begin{cases} L^*\phi_h = 0 \quad \text{in} \quad Q, \\ \phi_h(0,t) = \phi_h(1,t) = 0 \quad \text{on} \quad (0,T) \\ \phi_h(y,0) = I_{2h}^h(e_0), \ \ \phi_h'(y,0) = I_{2h}^h(e_1) \quad \text{in} \quad (0,1)\,. \end{cases}$$

– Considering that $\phi_{y,h}(0,t)$ is the derivative of the solution of the previous problem with respect to y, evaluated in $y = 0$, solve the following problem on the fine grid:

$$\begin{cases} L\psi_h = 0 \quad \text{in} \quad Q, \\ \psi_h(0,t) = -\phi_{y,h}(0,t), \ \ \psi_h(1,t) = 0 \quad \text{on} \quad (0,T) \\ \psi_h(y,T) = 0, \ \ \psi_h'(y,T) = 0 \quad \text{in} \quad (0,1)\,. \end{cases}$$

– Considering that $\phi_{y,h}(0,t)$ is the derivative of the solution of the previous problem with respect to y, evaluated in $y = 0$, solve the following problem on the fine grid:

$$\begin{cases} L\psi_h = 0 \quad \text{in} \quad Q, \\ \psi_h(0,t) = -\phi_{y,h}(0,t), \ \ \psi_h(1,t) = 0 \quad \text{on} \quad (0,T) \\ \psi_h(y,T) = 0, \ \ \psi_h'(y,T) = 0 \quad \text{in} \quad (0,1)\,. \end{cases}$$

– Remembering that v_0 and v_1 are the initial data of our problem after the change of variables and $I_h^{2h}(\psi_h) = \psi_{2h}$, calculate $g_0 = \left\{g_0^0, g_0^1\right\}$ on the less refined grid:

$$\begin{cases} -\Delta g_0^0 = \psi_{2h}'(0) + b(0)\psi_{y,2h}(0) - I_h^{2h}(v_1) - b(0) I_h^{2h}\left((v_0)_y\right). \\ g(0) = g(1) = 0. \end{cases}$$

$$g_0^1 = I_h^{2h} v_0 - \psi_{2h}(0)$$

– Define on the less refined (coarse) grid $w_0 = \left\{w_0^0, w_0^1\right\}$:

$$w_0^0 = g_0^0, \quad w_0^1 = g_0^1$$

$$\bar{g}_n^1 = -\bar{\psi}_{2h}(0)$$

- Step 1: For $n = 0, 1, 2, \ldots$

– Solve on the fine grid:

$$\begin{cases} L^*\bar{\phi}_h = 0 \quad \text{in} \quad Q, \\ \bar{\phi}_h(0,t) = \bar{\phi}_h(1,t) = 0 \quad \text{on} \quad (0,T) \\ \bar{\phi}_h(y,0) = I_{2h}^h(w_n^0), \ \ \bar{\phi'}_h(y,0) = I_{2h}^h(w_n^1) \quad \text{in} \quad (0,1)\,. \end{cases} \tag{5.1}$$

– Considering that $\bar{\phi}_{y,h}(0,t)$ is the derivative of the solution of the above problem with respect to y and evaluated in $y = 0$, solve the following problem on the fine grid:

$$\begin{cases} L\bar{\psi}_h = 0 \quad \text{in} \quad Q, \\ \bar{\psi}_h(0,t) = -\bar{\phi}_{y,h}(0,t), \ \ \bar{\psi}_h(1,t) = 0 \quad \text{on} \quad (0,T) \\ \bar{\psi}_h(y,T) = 0, \ \ \bar{\psi'}_h(y,T) = 0 \quad \text{in} \quad (0,1)\,. \end{cases}$$

– Calculate $g_n = \{g_n^0, g_n^1\}$ on the less refined grid:

$$\begin{cases} -\Delta \bar{g}_n^0 = \bar{\psi}'_{2h}(0) + b(0)\bar{\psi}_{y,2h}(0) \\ \bar{g}_n(0) = \bar{g}_n(1) = 0. \end{cases}$$

– Remembering that $F = H_0^1(0,1) \times L^2(0,1)$, calculate:

$$\rho = \frac{\|g_n\|_F^2}{(\bar{g}_n, w_n)_F}$$

– Calculate on the less refined (coarse) grid:

$$e_{n+1} = e_n - \rho w_n$$
$$\psi_{2h} = \psi_{2h} - \rho \bar{\psi}_{2h}$$
$$g_{n+1} = g_n - \rho \bar{g}_n$$

– Compute the residue:

$$residue = \frac{\|g_{n+1}\|_F^2}{\|g_0\|_F^2}$$

– Test of convergence: If $residue \leq \varepsilon$, stop and take $\psi = \psi_{2h}$. Otherwise, compute:

$$\gamma = \frac{\|g_{n+1}\|_F^2}{\|g_n\|_F^2}$$

– Calculate:

$$w_{n+1} = g_{n+1} + \gamma w_n$$

– Set $n = n + 1$ and go to (5.1).

6. Results: Numerical Simulations

The implementation of the algorithm we created, and that was presented above, was done using the software *MatLab*® 2016*a*. Further details can be found in the comments that are written with the code. Besides, the program we created is available on [22].

This section is devoted to the presentation and discussion of some numerical simulations that were performed, considering different moving boundaries and initial data. Once chosen the boundary and the initial data, we are interested in comparing the results of the simulations with and without the Bi-Grid method.

Let $U(T) = U(h : h : 1-h, T)$ be the vector that has the numerical position in all internal nodes (defined in the cylindrical domain) at the final time T as its coordinates. Similarly, $V(T) = V(h : h : 1-h, T)$ represents the vector that has the numerical velocity calculated at the final time T in all internal nodes as coordinates. In the following Tables, for each combination of input data, we will show, respectively, vertically, the results $\|U(T)\|_\infty$, $\|V(T)\|_\infty$ and the number of iterations performed.

Besides, it is worth mentioning that the value h corresponds to the discretization parameter of the fine spatial mesh (or of the unique one, when the Bi-Grid is not being used).

In addition, in this section, consider the following pairs of initial data:

(a) $v_0(y) = \sin^4(\pi y)\sin(5\pi y), \quad v_1(y) = 0$

(b) $v_0(y) = 0, \quad v_1(y) = \begin{cases} -y, \ y \in [0, 0.5], \\ 1 - y, \ \text{otherwise.} \end{cases}$

This way, in the subsequent subsections, we will discuss the results of numerical simulations for different examples of moving boundaries, including those that do not satisfy the hypotheses (2.5), (2.6) and (2.7) of Theorem 3.1.

6.1. Example 1 - Linear Boundary

In this subsection, we will study a linear moving boundary, given by:

$$\alpha(t) = \alpha_0 - \alpha_1 t, \quad \beta(t) = \beta_0 + \beta_1 t, \quad \forall t \in [0,T]\,,\ 0 < \alpha_1, \beta_1 \leq (\tau_0/2m)^{\frac{1}{2}}\,. \tag{6.1}$$

Note that the restriction $0 < \alpha_1, \beta_1 \leq (\tau_0/2m)^{\frac{1}{2}}$ appears to make sure that the hypotheses (2.5), (2.6) and (2.7) of Theorem 3.1 are satisfied. In addition to this, it holds that $\gamma(t) = (\beta_0 - \alpha_0) + (\beta_1 + \alpha_1)t$, then $(\beta_0 - \alpha_0) \leq \gamma(t)$ and the boundary grows smoothly.

In particular, taking $\alpha(t) = -1 - 10^{-2}t$, $\beta(t) = 1 + 10^{-2}t$, and $T = 16$, one can see its graph in Figure 4.

First, we want to investigate how the solution behaves when we increase α_1 and β_1, that is, the inclination of the boundary lines. For this, we will fix $\alpha_0 = -1$, $\beta_0 = 1$, so $\gamma(0) = 2$ (in other words, the length of the boundary at the initial time $t = 0$). We also set $T = 16$, $h = 2^{-8}$, $\Delta t = 0.5h$, mass $m = 1$,$\tau_0 = 8$, $k = 1$, $\sigma = 1$, the maximum number of iterations is 5000 and tolerance $\epsilon = 10^{-7}$. In Table 1, we analyze the behavior of the solution when increased the length of the boundary by $0\%, 2\%, 4\%, 8\%, 16\%, 32\%, 64\%$ and 128%, respectively. Note that, in these scenarios$\gamma(t)$ varies in $[2,2]$, $[2, 2.04]$, $[2, 2.08]$, $[2, 2.16]$, $[2, 2.32]$, $[2, 2.64]$, $[2, 3.28]$ and $[2, 4.56]$, respectively, remembering that $T = 16$, $\alpha_0 = -1$ and $\beta_0 = 1$.

As we will see later on, the case $\alpha_1 = \beta_1 = 0$ corresponds to the fixed domain for which not all the hypotheses of the Theorem 3.1 are verified and there is nothing we can guarantee about the numerical convergence. The choice $\alpha_1 = \beta_1 = \frac{1}{8} \times 10^{-2}$ results in a small boundary growth in the interval $[0,T]$, which can lead to coordinates of the final velocity vector not too close to zero, when using Bi-Grid. Since in this case, we have $\gamma(T) = 2.04$, it is believed that the behavior of this boundary is similar to the case of the fixed domain. Note that the in all simulations of Table 1, either with or without Bi-Grid, the position at the final time T was close to zero. The extreme case, that is, increasing a lot the inclination of the lines, also brings important changes to the numerical solution. In this case, when increasing the parameters α_1 and β_1, for example, taking $\alpha_1 = \beta_1 = 8 \times 10^{-2}$,the numerical simulations without Bi-Grid do not reach the tolerance ϵ under the maximum number of iterations set. In the other simulations, note that, in general, the results obtained without Bi-Grid were better, that is, closer to zero, than the ones with the Bi-Grid strategy, however, the number of iterations performed was much higher.

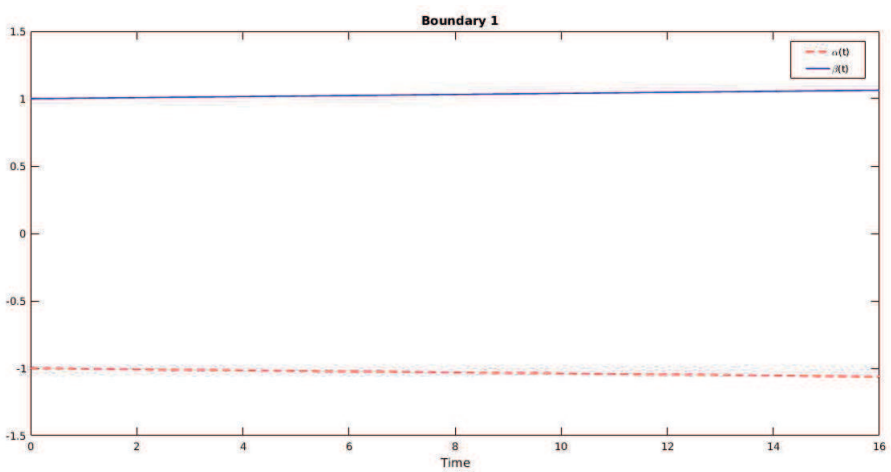

Figure 4: Linear boundary, taking $\alpha(t) = -1 - 10^{-2}t$, $\beta(t) = 1 + 10^{-2}t$ and $T = 16$.

Table 1: Example 1 - Linear boundary - Numerical Simulations varying the parameters $\alpha_1 = \beta_1$ and taking: $\alpha_0 = -1$, $\beta_0 = 1$, $T = 16$, $h = 2^{-8}$, $\Delta t = 0.5h$, $m = 1$, $\tau_0 = 8$, $k = 1$, $\sigma = 1$, $\epsilon = 10^{-7}$ and the maximum number of iterations is 5000.

	(a)		(b)	
$\alpha_1 = \beta_1$	With Bi-Grid	Without Bi-Grid	With Bi-Grid	Without Bi-Grid
0	7.76651×10^{-3}	4.46292×10^{-8}	7.78700×10^{-4}	3.70543×10^{-9}
	0.743156	3.72202×10^{-5}	8.10166×10^{-2}	3.42016×10^{-6}
	13	617	13	1091
$\frac{1}{8} \times 10^{-2}$	4.57247×10^{-3}	4.06018×10^{-8}	6.86334×10^{-4}	4.26499×10^{-9}
	0.4831692	3.64475×10^{-5}	9.99731×10^{-2}	3.33500×10^{-6}
	13	808	14	1169
$\frac{1}{4} \times 10^{-2}$	5.42260×10^{-4}	5.30920×10^{-8}	8.58139×10^{-4}	3.87664×10^{-9}
	5.72271×10^{-2}	3.54342×10^{-5}	8.99512×10^{-2}	3.02005×10^{-6}
	11	288	13	1690
$\frac{1}{2} \times 10^{-2}$	2.62931×10^{-4}	3.91033×10^{-8}	1.11770×10^{-3}	4.88946×10^{-9}
	2.88594×10^{-2}	2.84564×10^{-5}	9.38399×10^{-2}	3.92433×10^{-6}
	11	265	14	1779
1×10^{-2}	9.08392×10^{-5}	6.44533×10^{-8}	1.22595×10^{-3}	4.99204×10^{-9}
	4.63587×10^{-3}	3.54882×10^{-5}	7.88235×10^{-2}	3.65167×10^{-6}
	11	50	14	1982
2×10^{-2}	4.73535×10^{-4}	3.83148×10^{-8}	1.11491×10^{-3}	5.30125×10^{-9}
	2.54426×10^{-2}	3.27543×10^{-5}	7.34788×10^{-2}	3.49408×10^{-6}
	11	265	14	2689
4×10^{-2}	5.41088×10^{-4}	5.38975×10^{-8}	1.09987×10^{-3}	
	3.66034×10^{-2}	2.89455×10^{-5}	5.41369×10^{-2}	No convergence
	12	292	14	
8×10^{-2}	1.02062×10^{-3}		8.66085×10^{-4}	
	4.56311×10^{-2}	No convergence	3.94017×10^{-2}	No convergence
	13		15	

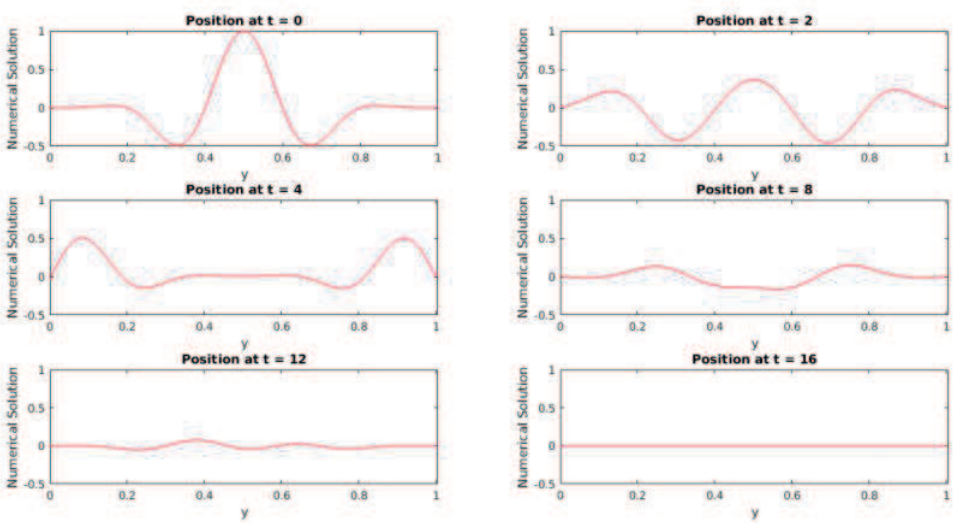

Figure 5: Position: numerical solution - initial data (a) with Bi-Grid

Considering the parameters from Table 1, Figure 5 shows the vibration of this string at different

discrete times for the simulation with Bi-Grid, taking $\alpha_1 = \beta_1 = 10^{-2}$ and initial data (a). Note that the vibrations cease due to the act of the control and at the final time (in this case, $T = 16$), the numerical position is close to the exact solution, that is, $y(T) = 0$.

In Figures 6 and 7, we can observe the behavior of the numerical control and numerical solution of our main problem, considering the pairs (a) and (b) of initial data, respectively, with and without Bi-Grid. These graphs show the results given by the program when taking the data of the simulations indicated in the fifth line of Table 1 ($\alpha_1 = \beta_1 = 10^{-2}$).

In particular, note that in Figure 7, the numerical control obtained in the scenario without Bi-Grid presents a lot of noise, and the same does not happen when Bi-Grid is taken under consideration.

For curiosity, it took the program 37276.76 seconds (that is, approximately, 10.35 hours) to calculate 1982 iterations of the simulation performed without Bi-Grid, taking the initial data (b), $\alpha_1 = \beta_1 = 10^{-2}$ and the other information mentioned in Table 1. The computer used has 16 GB of RAM memory and a I7-7700K processor.

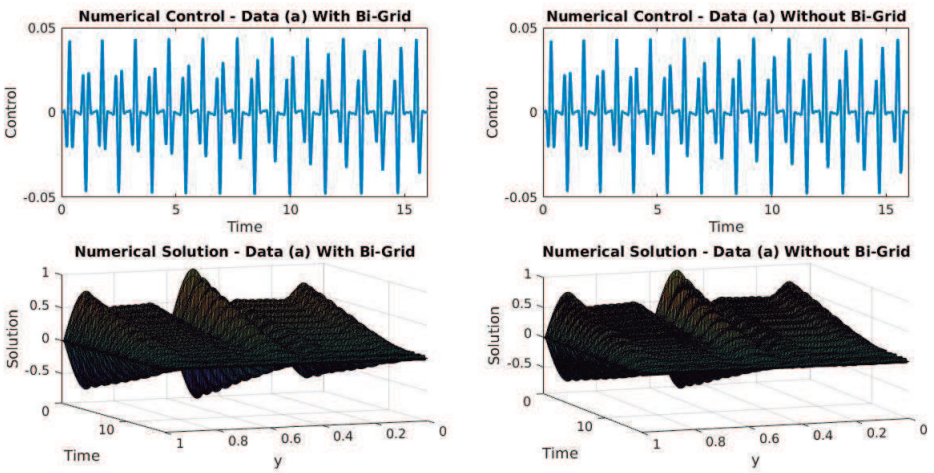

Figure 6: Numerical Simulation and Control - Initial Data(a): With Bi-Grid $\times$ Without Bi-Grid

Now, we want to analyse what happens when the final time T changes. For this, take at look at Table 2, in which we set $\alpha(t) = -1 - 10^{-2}t$, $\beta(t) = 1 + 10^{-2}t$ and the parameters $m = 1$, $\tau_0 = 8$, $k = 1$, $\sigma = 1$, $h = 2^{-8}$, $\Delta t = 0.5h$, $\epsilon = 10^{-7}$ and the maximum number of iterations is 2000. At first, note that for $T = 4$ and $T = 8$, we have that $T < 2/\sqrt{k_0}$, that is, this choices of values does not satisfy one of the hypotheses of Theorem 3.1 and as the simulations show, there is nothing we can affirm. For the other values of T used in Table 2, once we choose the initial pair of data and a big enough final time T and decide either using the Bi-Grid strategy or not, considering a larger time does not significantly change the position and velocity at T. Once again, observe that many more iterations are performed to reach the tolerance ϵ in the scenario without Bi-Grid and this number of iterations does not follow any pattern.

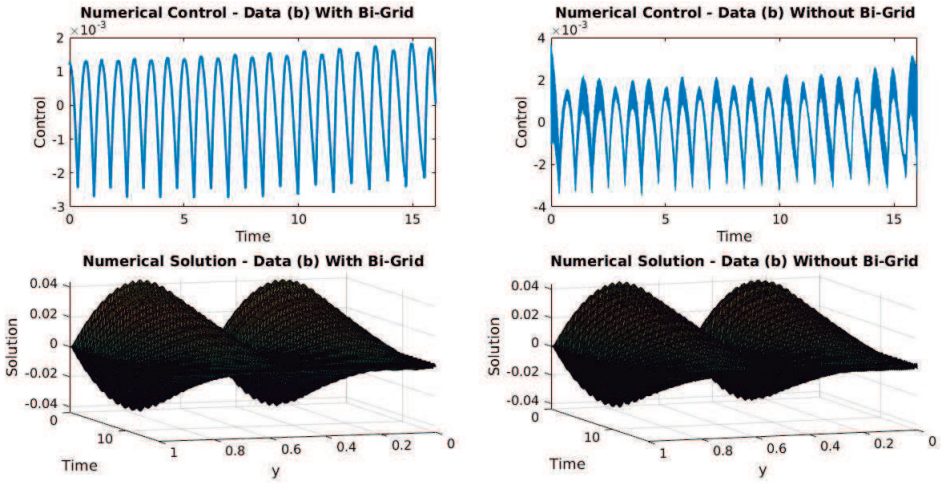

Figure 7: Numerical Simulation and Control - Initial Data(b): With Bi-Grid × Without Bi-Grid

Table 2: Linear boundary given by $\alpha(t) = -1 - 10^{-2}t = -\beta(t)$. Numerical simulations varying T, considering: $h = 2^{-8}$, $\Delta t = 0.5h$, $m = 1$, $\tau_0 = 8$, $k = 1$, $\sigma = 1$, $\epsilon = 10^{-7}$ and the maximum number of iterations is 2000.

	(a)		(b)	
T	With Bi-Grid	Without Bi-Grid	With Bi-Grid	Without Bi-Grid
4	2.72566×10^{-2}		1.64401×10^{-3}	
	3.18925	No convergence	2.00959×10^{-1}	No convergence
	17		17	
8	3.04286×10^{-4}	5.14690×10^{-8}	8.36974×10^{-4}	
	2.61374×10^{-2}	2.60684×10^{-5}	9.97656×10^{-2}	No convergence
	11	448	15	
16	9.08392×10^{-5}	6.44533×10^{-8}	1.22595×10^{-3}	4.99204×10^{-9}
	4.63587×10^{-3}	3.54882×10^{-5}	7.88235×10^{-2}	3.65167×10^{-6}
	11	50	14	1982
40	5.67985×10^{-5}	6.35446×10^{-8}	7.28874×10^{-4}	5.54476×10^{-9}
	4.51391×10^{-3}	3.00133×10^{-5}	5.31537×10^{-2}	3.11512×10^{-6}
	10	161	13	422
64	2.95595×10^{-4}	3.35694×10^{-8}	6.98604×10^{-4}	4.85572×10^{-8}
	1.65598×10^{-2}	1.90966×10^{-5}	5.70521×10^{-2}	3.00278×10^{-6}
	11	225	13	359

Numerical simulations were also performed keeping the same initial parameters used in the previous simulations and varying Δt, that is, $\Delta t = \mu h$, for $\mu = 1,\ 0.5,\ 0.25,\ 0.1$. They showed that these values do not significantly change the numerical solution. This way, we will continue taking $\mu = 0.5$ on the next examples.

Table 3: Linear Boundary $\alpha(t) = -1 - 10^{-2}t = -\beta(t)$: Variation of ϵ and h with Bi-Grid, considering pair (a) of initial data and: $T = 16$, $\Delta t = 0.5h$, $m = 1$,$\tau_0 = 8$, $k = 1$, $\sigma = 1$.

$\epsilon \setminus h$	2^{-6}	2^{-7}	2^{-8}	2^{-9}	2^{-10}
10^{-4}	1.54587×10^{-3}	3.97209×10^{-4}	9.51196×10^{-5}	3.89026×10^{-5}	3.23973×10^{-5}
	1.01497×10^{-1}	1.42745×10^{-2}	5.66903×10^{-3}	6.80744×10^{-3}	1.61008×10^{-2}
	6	6	5	5	4
10^{-5}	1.54631×10^{-3}	3.97954×10^{-4}	9.07658×10^{-5}	3.53713×10^{-5}	1.95612×10^{-5}
	1.01744×10^{-1}	1.31543×10^{-2}	4.57909×10^{-3}	3.19360×10^{-3}	3.80433×10^{-3}
	8	8	7	7	7
10^{-6}	1.54645×10^{-3}	3.97875×10^{-4}	9.08530×10^{-5}	3.58526×10^{-5}	1.77896×10^{-5}
	1.01720×10^{-1}	1.31789×10^{-2}	4.63828×10^{-3}	3.08089×10^{-3}	3.52146×10^{-3}
	9	9	9	8	8
10^{-7}	1.54639×10^{-3}	3.97886×10^{-4}	9.08399×10^{-5}	3.58965×10^{-5}	1.76322×10^{-5}
	1.01711×10^{-1}	1.31757×10^{-2}	4.63587×10^{-3}	3.11023×10^{-3}	3.40351×10^{-3}
	12	11	11	10	10
10^{-8}	1.54640×10^{-3}	3.97890×10^{-4}	9.08399×10^{-5}	3.58908×10^{-5}	1.75890×10^{-5}
	1.01712×10^{-1}	1.31764×10^{-2}	4.63687×10^{-3}	3.10835×10^{-3}	3.40343×10^{-3}
	14	13	12	12	12
10^{-9}	1.54640×10^{-3}	3.97891×10^{-4}	9.08390×10^{-5}	3.58908×10^{-5}	1.75934×10^{-5}
	1.01712×10^{-1}	1.31762×10^{-2}	4.63672×10^{-3}	3.10902×10^{-3}	3.40349×10^{-3}
	16	15	15	15	14
10^{-10}	1.54640×10^{-3}	3.97891×10^{-4}	9.08390×10^{-5}	3.58908×10^{-5}	1.75950×10^{-5}
	1.01712×10^{-1}	1.31762×10^{-2}	4.63673×10^{-3}	3.10904×10^{-3}	3.40332×10^{-3}
	18	17	16	16	16

Table 4: Linear boundary $\alpha(t) = -1 - 10^{-2}t = -\beta(t)$: Variation of ϵ and h without Bi-Grid, considering pair (a) of initial data and: $T = 16$, $\Delta t = 0.5h$, $m = 1$,$\tau_0 = 8$, $k = 1$, $\sigma = 1$.

$\epsilon \setminus h$	2^{-6}	2^{-7}	2^{-8}	2^{-9}	2^{-10}
10^{-4}	1.3173×10^{-5}	1.1130×10^{-5}	1.1644×10^{-5}	1.1193×10^{-5}	1.0951×10^{-5}
	1.7297×10^{-3}	7.6007×10^{-4}	1.0628×10^{-3}	1.0659×10^{-3}	1.7519×10^{-3}
	4	4	4	4	4
10^{-5}	4.5360×10^{-6}	1.3079×10^{-6}	1.5267×10^{-6}	1.9337×10^{-6}	1.8199×10^{-6}
	1.0279×10^{-3}	4.5429×10^{-4}	6.4729×10^{-4}	6.4991×10^{-4}	8.7849×10^{-4}
	5	5	5	5	5
10^{-6}	4.1596×10^{-7}	5.7667×10^{-7}	1.0034×10^{-6}	1.4657×10^{-6}	1.1136×10^{-6}
	1.0152×10^{-4}	1.2222×10^{-4}	2.7380×10^{-4}	5.4229×10^{-4}	7.0839×10^{-4}
	23	9	7	6	6
10^{-7}	4.2726×10^{-8}	5.6779×10^{-8}	6.4453×10^{-8}	6.5513×10^{-8}	9.2004×10^{-8}
	6.8399×10^{-6}	1.3089×10^{-5}	3.5488×10^{-5}	8.5702×10^{-5}	2.5238×10^{-4}
	58	94	50	115	54
10^{-8}	4.7436×10^{-9}	4.3984×10^{-9}	4.6359×10^{-9}	5.5174×10^{-9}	8.0108×10^{-9}
	4.3092×10^{-7}	1.4831×10^{-6}	3.4095×10^{-6}	6.6887×10^{-6}	1.8771×10^{-5}
	98	187	266	352	338
10^{-9}	3.2197×10^{-10}	3.8141×10^{-10}	3.8011×10^{-10}	5.3088×10^{-10}	6.3610×10^{-10}
	3.4383×10^{-8}	1.0767×10^{-7}	2.7850×10^{-7}	7.6671×10^{-7}	1.2885×10^{-6}
	106	209	1298	904	1908
10^{-10}	4.2614×10^{-11}	5.1313×10^{-11}	6.5674×10^{-11}	6.7992×10^{-11}	5.7633×10^{-11}
	7.3858×10^{-9}	1.6252×10^{-8}	3.4090×10^{-8}	6.9227×10^{-8}	1.2539×10^{-7}
	133	247	1351	2738	6349

Finally, we want to investigate the relationship between the spatial increment h and the tolerance ϵ. In Table 3, we can find the results obtained when considering the Bi-Grid technique, pair of initial data (a), linear boundary given by $\alpha(t) = -1 - 10^{-2}t = -\beta(t)$ and $T = 16$, $\Delta t = 0.5h$, $m = 1$, $\tau_0 = 8$, $k = 1$, $\sigma = 1$. Note that once h is fixed, the chosen value of ϵ does not significantly change the values obtained for the largest entry, in modulus, of vectors position and velocity at the final time T. On the other hand, when setting ϵ, in order to get better results, it is necessary to choose a smaller h, that is, deal with a finer mesh.

The behavior described above does not occur when considering the same data, but without the Bi-Grid strategy, as shown in Table 4. In this case, once fixed the parameter ϵ, working with a finer mesh practically does not entail changes in the largest input, in modulus, of the position and velocity vectors at the final time T. On the other hand, once h is fixed, in order to obtain final position and velocity vectors closer to the null one, it is necessary to take smaller values of ϵ. Note that when refining the mesh and decreasing the tolerance parameter, we get high numbers of iterations, larger than the ones in Table 3. One more time, comparing numerical simulations with the same initial data either with or without Bi-Grid, once there is convergence in both cases, the scenario without Bi-Grid will return final position and velocity vectors closer to the null one, however, for this, a greater number of iterations will be performed.

7. Discussion : Questioning the hypotheses

In this subsection, the consistency of the properties of the theoretical results and the numerical ones will be analyzed. In order to verify what happens when at least one hypothesis of Theorem 3.1 is not satisfied, in this subsection, we will analyze the results of numerical simulations, considering two examples of boundaries under these conditions.

7.1. Example 2 - Fixed domain

In this example, we will consider the cylindrical domain, that is:

$$\alpha(t) = 0, \quad \beta(t) = 1, \quad \forall t \in [0, T]\,. \tag{7.1}$$

Notice that this choice of boundary is not under the hypotheses of Theorem 3.1, because, for instance, (2.7) is not verified.

First, we will take different pairs of initial data, and the following parameters are fixed: $T = 16$, the step of fine space mesh is $h = 2^{-8}$, time step is $\Delta t = 0.5h$, constant $m = 1$, initial tension is $\tau_0 = 1$, constant $k = 5$, $\sigma = 1$ and tolerance parameter is $\epsilon = 10^{-7}$. Note that the choice $T = 16$ satisfy the hypothesis of Theorem 3.1, that is, it is true that $T > 2/\sqrt{k_0}$. The results of the numerical simulations performed can be found in Table 5. Analysing it, we can notice that, using the Bi-Grid strategy, the final velocity of the numerical simulations in lines 2 and 4 are not close to 0, as desired. The same situation does not occur when Bi-Grid is not taken under consideration. In this case, more iterations were performed, however, the final position and velocity are close to zero. Therefore, there is nothing one can guarantee about the convergence when all the hypotheses of Theorem 3.1 are not satisfied.

Table 5: Fixed domain - Numerical simulations, considering different pairs of initial data and: $T = 16$, $h = 2^{-8}$, $\Delta t = 0.5h$, $m = 1$,$\tau_0 = 1$, $k = 5$, $\sigma = 1$ and $\epsilon = 10^{-7}$.

$v_0(y)$	$v_1(y)$	With Bi-Grid	Without Bi-Grid
$\sin^4(\pi y)\sin(5\pi y)$	0	6.736943×10^{-4}	4.975338×10^{-8}
		3.738781×10^{-2}	4.071897×10^{-5}
		9	137
$\sin(2\pi y)$	0	1.783749×10^{-2}	1.354483×10^{-7}
		1.015848	6.214993×10^{-5}
		10	317
0	$\begin{cases} -y, & y \in [0, 0.5], \\ 1 - y, & \text{otherwise.} \end{cases}$	1.759535×10^{-3}	4.688007×10^{-9}
		7.225315×10^{-2}	2.131589×10^{-6}
		11	477
$\begin{cases} 2y, & y \in [0, 0.5], \\ 0, & \text{c. c.} \end{cases}$	0	6.168681×10^{-2}	5.998667×10^{-8}
		36.034067	2.605271×10^{-5}
		11	513

Table 6: Fixed domain - Numerical simulations, varying T and considering: $h = 2^{-8}$, $\Delta t = 0.5h$, $m = 1$,$\tau_0 = 1$, $k = 5$, $\sigma = 1$, $\epsilon = 10^{-7}$ and the maximum number of iterations is 1000.

	$v_0(y) = \sin^4(\pi y)\sin(5\pi y), \quad v_1(y) = 0$		$v_0(y) = 0, \quad v_1(y) = \begin{cases} -y, \ y \in [0, 0.5], \\ 1 - y, \ \text{c.c.} \end{cases}$	
T	With Bi-Grid	Without Bi-Grid	With Bi-Grid	Without Bi-Grid
4	8.782309×10^{-4}	9.112170×10^{-8}	2.051600×10^{-3}	No convergence
	5.340690×10^{-2}	3.444755×10^{-5}	1.928093×10^{-1}	
	10	311	13	
8	4.946449×10^{-4}	5.291793×10^{-8}	1.924194×10^{-3}	No convergence
	3.692336×10^{-2}	2.242812×10^{-5}	1.143134×10^{-1}	
	9	242	12	
16	6.736943×10^{-4}	4.975338×10^{-8}	1.759535×10^{-3}	4.688007×10^{-9}
	3.738781×10^{-2}	4.071897×10^{-5}	7.225315×10^{-2}	2.131589×10^{-6}
	9	137	11	477
32	8.660646×10^{-4}	2.04160×10^{-8}	1.540664×10^{-3}	6.677809×10^{-9}
	6.489804×10^{-2}	1.854811×10^{-5}	8.196468×10^{-2}	2.834062×10^{-6}
	9	144	11	145

Now, we want to investigate how the final time T affects the simulations. For this, we will vary T, once fixed all the other parameters, that is, $h = 2^{-8}$, $\Delta t = 0.5h$, $m = 1$, $\tau_0 = 1$, $k = 5$, $\sigma = 1$, the maximum number of iterations is 1000 and $\epsilon = 10^{-7}$. We will consider values of T that satisfy the hypothesis $T > 2/\sqrt{k_0}$ and other that don't. The results of these new simulations can be found in Table 6. Note that for $T = 4$ and $T = 8$, this already mentioned hypothesis is not verified. The same behavior happens when taking other values less than $2/\sqrt{k_0}$, for instance, $T = 2$. Besides, for the second pair of initial data, (b), there was no convergence, considering the tolerance ϵ given. One can also observe that, when there was convergence, the results without Bi-Grid were closer to zero, but a greater number of iterations was needed.

Even though they don't appear in Table 6, other simulations where performed considering different values $T > 2/\sqrt{k_0}$, for instance, $T = 64$ and the same behavior as the one shown $T = 16$ and $T = 32$ was detected. Finally, we can conclude that if $T > 2\sqrt{k_0}$, increasing T will not bring significant changes to the final position and velocity.

7.2. Example 3

In this example, we consider:

$$\alpha(t) = \frac{1}{2}\left(cos\frac{2\pi t}{T} - 1\right), \quad \beta(t) = \frac{1}{2}\left(3 - cos\frac{2\pi t}{T}\right). \tag{7.2}$$

Note that this choice of moving boundary does not satisfy $\alpha^{'}(t) < 0 < \beta^{'}(t)$, $\forall t \in [0, T]$. In particular, $T = 16$ and $T = 36$ satisfy the hypothesis $T > 2/\sqrt{k_0}$. Its graph can be seen in Figure 8.

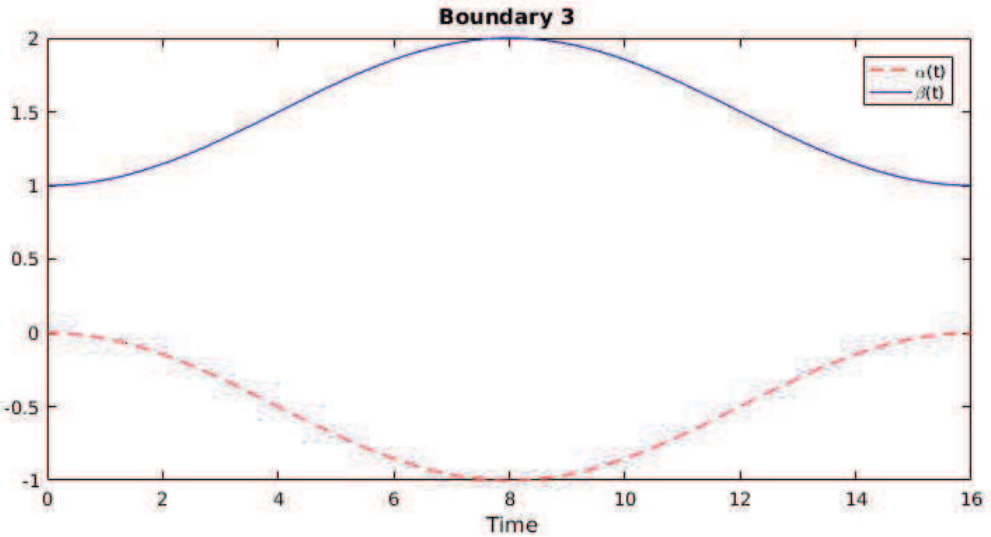

Figure 8: Moving boundary - Example 3

Similar behavior occurs when $T = 36$ and it also satisfies $T > 2/\sqrt{k_0}$. Nevertheless, we will conduct numerical simulations considering this boundary example and different pairs of initial position and velocity, and $T = 36$, $h = 2^{-8}$, $\Delta t = 0.5h$, $m = 1$, $\tau_0 = 9$, $k = 5$, $\sigma = 1$, $\epsilon = 10^{-5}$ and the maximum number of iterations is 1100. The results can be found in Table 7. Observe that the results of the first three simulations of this Table are good whether using Bi-Grid or not. However, analysing the last pair of initial data considering the Bi-Grid strategy, the largest input of the final speed, in module, is large, that is, distant from 0. As for the case without Bi-Grid, the simulation did not reach the precision ϵ given. Therefore, once again, there's nothing one can affirm about the convergence when the hypotheses of Theorem 3.1 are not satisfied.

Table 7: Moving boundary - Example 3 - Numerical simulations with different initial data and: $T = 36$, $h = 2^{-8}$, $\Delta t = 0.5h$, $m = 1$,$\tau_0 = 9$, $k = 5$, $\sigma = 1$, $\epsilon = 10^{-5}$ and the maximum number of iterations is 1100.

$v_0(y)$	$v_1(y)$	With Bi-Grid	Without Bi-Grid
$\sin^4(\pi y)\sin(5\pi y)$	0	3.342328×10^{-4}	5.808802×10^{-6}
		7.684647×10^{-2}	3.293442×10^{-3}
		8	122
$\sin(2\pi y)$	0	4.247025×10^{-4}	1.269178×10^{-5}
		9.821907×10^{-2}	6.223536×10^{-3}
		11	44
0	$\begin{cases} -y, \ y \in [0, 0.5], \\ 1 - y, \ \text{c.c.} \end{cases}$	5.127436×10^{-4}	3.193424×10^{-7}
		5.413099×10^{-2}	4.241180×10^{-4}
		9	1022
$\begin{cases} 2y, \ y \in [0, 0.5], \\ 0, \ \text{c. c.} \end{cases}$	0	6.427781×10^{-2}	No convergence
		1.129407×10^{2}	
		10	

In conclusion, after analysing the numerical simulations presented in this section, we realized that when we are not under the assumptions of Theorem 3.1, there is nothing one can guarantee about the numerical convergence, because it will depend on the initial data. We also noticed that there are some combinations of initial data for which the numerical simulations without Bi-Grid do not converge, once

fixed the parameter ϵ. However, the same thing does not happen when the Bi-Grid technique has been taken under consideration. Besides, in cases where there was convergence with and without Bi-Grid, the results obtained without it were better (that is, position and velocity at the final time are closer to zero), however, a greater number of iterations was needed.

8. Conclusions

In this work, we developed (and shared [22]) a numerical method to obtain an exact approximate control for the mathematical model, which describes the vertical vibrations of an elastic string with moving boundary, proposed by [1]. We showed that the numerical results obtained are consistent with the theoretical results. However, in general, important properties can be lost when spatial and temporal discretization parameters tends to zero. For the determination of the exact control, the Bi-Grid technique had fundamental importance, as shown in the numerical simulations.

Acknowledgements

The author C. E.O. Moraes is partially supported by CAPES and M.A. Rincon is partially supported from CNPq research (Grant: 301571/2019-8) and FAPERJ(Grant: CNE 2022/2025)-Brazil .

References

1. Araruna, F.D.; Medeiros, L. A.; Antunes, G.: *Exact controllability for the semilinear string equation in non cylindrical domains*. Control and Cybernetics, [S.l.], v. 33, n. 2, p. 237-257, 2004.

2. Araruna, F. D. ; Chaves-Silva, F. W. ; Rojas-Medar, M. A. . *Exact Controllability of Galerkin's Approximations of Micropolar Fluids*. Proceedings of the American Mathematical Society, v. 138, p. 1361-1370, 2010.

3. Araujo de Souza, Diego *Resultados teóricos y numéricos de control para EDPs lineales y no lineales*. Universidad de Sevilla. Phs Thesis (2015) http://hdl.handle.net/11441/25453

4. Capistrano-Filho, R, Pazoto, A., Rosier, L. *Internal controllability of the Korteweg-de Vries equation on a bounded domain*. ESAIM: COCV v.21, N.4, pg 1076-1107, (2015)

DOI:10.1051/cocv/2014059

5. Carreño, A, N. ; Santos, M.C. . *Stackelberg-Nash exact controllability for the Kuramoto-Sivashinsky equation.* Journal of Differential Equations, v. 266, p. 6068-6108, 2019.

6. Chaves-Silva, F. W.; Araujo de Souza, Diego:. *On the controllability of some equations of Sobolev-Galpern type*. Journal of Differential Equations, Vol.268, N^o4, pg.1633-1657,2020.

7. Chaves-Silva, F. W.: *A hyperbolic system and the cost of the null controllability for the Stokes system*. Computational & Applied Mathematics, v. 34, p. 1057-1074, 2015.

8. Chaves-Silva, Felipe W.; Rosier, L.; Zuazua, E. : *Null controllability of a system of viscoelasticity with a moving control.* Journal de Mathématiques Pures et Appliquées, v. 101, Issue 2, (2014), Pages 198-222

9. De Carvalho, P.P. :*Some numerical results for control of 3D heat equations using Nash equilibrium.* Comp. Appl. Math. 40, 92 (2021).

10. De Carvalho, P.P.; Límaco, J. ; Thamsten, Y. ; Menezes, D. :*Local null controllability of a class of non-Newtonian incompressible viscous fluids.* Evolution Equations and Control Theory, v. 1, p. 31, 2021.

11. Font, R.; Periago, F. *Numerical simulation of the boundary exact control for the system of linear elasticity*. Applied Mathematics Letters 23:1021-1026 (2010) DOI:10.1016/j.aml.2010.04.030

12. Glowinski, R.; Kinton,W.; Wheeler, M. F. A mixed finite element formulation for the boundary controllability of the wave equation. :*International Journal for Numerical Methods in Engineering*, Chichester, v. 27, n. 3, p. 623-635, 1989.

13. Glowinski, R.; Li, C.-H.; Lions, J.-L. A numerical approach to the exact boundary controllability of the wave equation (I). Dirichlet controls: Description of the numerical methods. :*Japan Journal of Applied Mathematics*, v. 7, n. 1, p. 1-76, 1990.

14. Glowinski, R. Ensuring well posedness by analogy; stokes problem and boundary control for the wave equation. :*Journal of Computational Physics*, Orlando, v. 103, n. 2, p. 189-221, 1992.

15. Kogut, P.I; Kupenko, O.P.; Leugering, G.*On boundary exact controllability of one-dimensional waveequations with weak and strong interior degeneration*. Math Meth Appl Sci. 2022;45:770–792

16. Borsch,V.L , Kogut, P.I.PI. *The exact bounded solutiontoan initial boundary value problem for 1-D hyperbolic equation with interior degeneracy.I. Separation of variables.* J Optim Diff Equ Appl (JODEA). 2020;28(2):2-20.25.

17. Límaco, J.; Nuñez-Chávez, M. R.; Huaman, D. N. Exact controllability for nonlocal and nonlinear hyperbolic PDEs, Nonlinear Analysis 214 (112569), 2022.

18. Lions, J. L. :*Controlalibilité exacte de systemes distribuées*, C. R. Acad. Sci., Paris, 302 (1986), 471-475.

19. Lions, J. L. :*Controlabilité exacte, pertubation et estabilization de systemes distribuées*: tome 1: controlabilité exacte. Paris: Masson, 1988.

20. Medeiros, L. A. da J.; Limaco, J.; Menezes, S. B. Vibrations of elastic strings: mathematical aspects, part 1 e part 2. :*Journal of Computational Analysis and Applications*. v. 4, n. 2, p. 97-127, 2002, v. 4, n. 3, p. 212-263, 2002.

21. Miranda, M. M. HUM and the wave equation with variable coefficients. :*Asymptotic Analysis*, Amsterdam, v. 11, n. 4, p. 317-341, 1995.

22. Moraes, C. E. O. de, Algorithm for the exact control of the elastic string problem with moving boundary. Last access: 01/29/2020. https://goo.gl/QCvUrr

23. Negreanu, M. : *Métodos numéricos para el análisis de la propagación, observación y control de ondas*. 2003. (PH.D Thesis) - Universidad Complutense de Madrid, Madrid, 2003.

24. Rincon, M. A.; Garay, M. Z.; Miranda, M. M. Numerical approximation of the exact control for the string equation. :*International Journal of Pure and Applied Mathematics*, [S.l.], v. 8, n. 3, p. 349-368, 2003.

25. Salem, A.: *Numerical approximation of exact controllability for Korteweg-de Vries equation.* AIP Conference Proceedings 1107, 231 (2009); https://doi.org/10.1063/1.3106478

Carla E. O. de Moraes,
PPGI- Universidade Federal do Rio de Janeiro - Brasil
E-mail address: carla.moraes@ppgi.ufrj.br

and

Mauro A Rincon,
Institute of Computng,
Universidade Federal do Rio de Janeiro - Brasil.
E-mail address: rincon@dcc.ufrj.br

and

Gladson O. Antunes,
EM-Universidade Federal do Estado do Rio de Janeiro - Brasil.
E-mail address: gladson.antunes@uniriotec.br